

Interphase Slipping Effect on Flame Propagation Characteristics in Micro-Iron Dust Particles

Mohsen Broumand, Saeed Shayamehr, Mehdi Bidabadi

Combustion Research Laboratory, School of Mechanical Engineering, Iran University of Science and Technology

Abstract

In this paper, the impact of interphase slipping (i.e., relative velocity between micro-iron dust particles suspended in air and surrounding gas flow) on flame propagation characteristics is studied. Initially, to obtain an explicit algebraic equation for the flame velocity, mass and energy conservation equations are solved. Then, dynamic equations of micro-iron particles during the upward flame propagation in a vertical duct are considered to calculate the particle velocities as a function of their distances from the leading edge of the flame. After that, by balancing the mass flux passing through a control volume above the leading edge of the flame, the change in the number density of the particles is determined. As a result, it is shown that due to the interphase slipping effect, mass concentration of micro-iron particles upon the leading edge of the flame is approximately twice as large as it is at a distance far from the flame. This accumulation causes flame moves in a denser dust cloud, which has a significant effect on the flame propagation characteristics such as flame velocity and temperature. The theoretical results show reasonable correlation with the experimental data.

Keywords: Micro-iron particles; Interphase slipping; Flame velocity; Mass concentration; Heterogeneous combustion

I. Introduction

Study on the combustion of dust/gas mixtures can be useful in many technological aspects such as dust explosion hazards management, fire suppression techniques, and fossil fuel combustion [1-4]. Aluminum powder is used in solid-fueled propulsion systems in order to boost the combustion enthalpy. It has been long that metal such as hafnium, titanium, zirconium and beryllium are used as energizing additives in propellants, incendiaries and flame synthesis. There are also many reasons supporting the importance of considering alternative energy carriers such as metal particles [5]. However, despite the importance of dust cloud combustion, developing a comprehensive theory for it is quite difficult. This notable feature is based on the fact that the heterogeneous combustion theory is not as well-established as the theory of homogeneous gas flames in which the mechanism of the combustion wave propagation is defined using physico-chemical characteristics of the reactive mixture.

Associating with the importance of dust explosion and flame propagation through dust clouds, Sun et al. [6-9] conducted some experiments to observe the combustion behavior of iron particles near the combustion zone across the upward and downward flame propagating and consequently, the velocity and number density profiles of particles were obtained from their researches. Cashdollar et al. [10,11] also performed some experiments to calculate the temperature and the pressure of dust mixtures at the time of explosion in a spherical chamber for both

metallic particles such as iron and non-metallic particles. Recently, Kosinski et al. [12] experimentally investigated the maximum explosion pressures and the maximum rates of pressure rise of hybrid mixtures as a function of carbon black and propane concentrations. As they noted, it is needed that further researchers conduct several studies for modeling of chemical reactions of such mixtures with regard to the possible particle-particle and particle-surface interactions.

In spite of the fact that a wide range of studies have already been carried out on the dust cloud combustion for various fuels such as coal, hydrocarbons, biomass and metal particles [13-17], the differences among them are striking, and they deserve thorough investigation. These differences originate from the following concepts: a) The interaction between the particles and the effect of that on the dust cloud combustion, b) The interaction between the surrounding gas and the particles and the effect of that on the process of dust cloud combustion, c) The interaction between the flame and the gas-particle mixture and the effect of that on the flame propagation. Therefore, in analyzing the premixed particle-cloud flames, the evaluation of the interaction between different phases is of the utmost importance. In this regard, Vainshtein and Nigmatulin [18] noted that the velocity of the gaseous phase significantly increases near the reaction zone of dust clouds because of the thermal expansion of the carrier gas. As they stated, the particle motion is completely determined by the

carrier gas motion and depends on the interphase friction force. The same phenomenon has been also observed during the combustion of coarse magnesium particles conducted by Dreizin and Hoffman [19]. They claimed that for an aerosol of coarse magnesium particles, particle motion due to drag forces was found to change the number density of articles in the unburned aerosol during the constant pressure flame propagation experiments. As they pointed, the increase in the number density of particles just ahead of the flame must influence the lower flammability limits of a combustible particle cloud.

Study on a nonvolatile metal such as iron, which burns in a condensed phase, is also prominent in evaluating the models demonstrating the heterogeneous characteristics of particles combustion [20,21]. The laminar flame propagation regime seems particularly interesting since, provided the experimental conditions are adequate, some important characteristics of the flame (i.e., laminar burning velocity, maximum flame temperature) should depend only on the mixture and seem good candidates for the definition of explosion parameters, which depend only on the nature of the mixture [22]. Accordingly, the main intention of the present study is a one-dimensional, steady-state theoretical analysis of flame propagation in a heterogeneous medium (i.e., micro-iron dust particles suspended in air) with a special remark on the impact of the relative velocity (i.e., interphase slipping).

In the present study, initially the temperature profile and flame propagation velocity through the mixture of micro-iron and air is calculated solving energy and mass conservation equations taking the appropriate boundary conditions into account. Then, the position and velocity of particles as functions of time, and also the profiles of particle velocities based on the position of particles are gained in the preheat zone. After that, the particles concentration in front of the flame and particularly on the leading edge of the flame is calculated according to the velocity difference between the surrounding gas flow and particles. Ultimately, calculations were accomplished by utilizing an actual mass concentration of particles instead of initial one to obtain more realistic estimates of the laminar flame velocity propagating in suspensions of iron dust in air. In this paper, the combustion chamber is assumed to be a vertical channel including a mobile wall. At first, the wall causes the combustion chamber to act as a closed combustion chamber. Iron particles are dispersed in the combustion chamber by air flow and then as soon as the wall goes down to the bottom of the chamber, the particles are ignited by means of a pair of electrodes. The produced flame begins moving upward through the micro-iron particles as it is illustrated in figure (1). Utilizing such combustion chamber has several advantages as shown by Sun et al. [6-9] and Han et al. [23].

II. Mathematical modeling

2.1. Dynamic equations of particles

The motion equation of a spherical particle relative to an infinite, stagnant and viscous fluid was first developed by Basset [24]. For a moving fluid, Basset's equation can be expressed as:

$$\frac{\pi d_p^3}{6} \rho_p \frac{dv_p}{dt} = -3\pi\mu d_p (v_p - v_F) + \frac{\pi d_p^3}{6} \rho_F \frac{dv_F}{dt} - \frac{1}{2} \frac{\pi d_p^3}{6} \rho_F \frac{d(v_p - v_F)}{dt} - \frac{3}{2} d_p^2 (\pi\mu\rho_F)^{1/2} \int_{t_0}^t \frac{d(v_p - v_F)}{d\xi} \frac{d\xi}{(t - \xi)^{1/2}} \quad (1)$$

Where d_p is the particle diameter, v the velocity, ρ the density, μ the fluid viscosity, t the time and subscripts p and F designate the particle and the fluid respectively. The term on the left indicates the accelerating force applied to the particle and the right one shows the Stokes drag force, the pressure gradient force on fluid, fluid resistance to accelerating sphere and drag force associated with unsteady motion respectively. In addition to the above-mentioned forces, there might be other forces acting on the particle such as gravitation, centrifugal, electromagnetic, thermophoretic, diffusiphoretic, and Brownian forces, etc.

In general, in gas and metal particle mixtures, the forces involving ρ_F compared to the forces involving ρ_p can be ignored. This is because the particles density is many orders of magnitude larger than the fluid density. In most combustion environments, centrifugal and electromagnetic forces do not exist. And in the absence of high concentration gradients in the system, diffusiphoretic force can also be ignored. However, the thermophoretic forces and gravitation forces have major effects on the motion of particles and a deeper study is felt required. The Brownian forces in system are resulted from the collisions between the fluid molecules and fine particles, which play a crucial role for the small particles and are usually dominated by other forces. As a result, the following equation is obtained for the combustion of metal dust particles.

$$m_p \frac{dv_p}{dt} = F_D + F_G + F_B + F_T \quad (2)$$

In which v_p, m_p are the particle velocity and mass.

Besides, $F_T, F_B, F_G,$ and F_D are thermophoretic, buoyancy, gravitation and drag forces respectively. These forces will be described in more detail in the following sections.

2.1.1. Drag force

This force is resulted from the difference between the velocity of a particle and the gases in its

surrounding environment. In general, the drag coefficient depends on the shape and the orientation of a particle with respect to the flow and must be calculated considering the flow parameters such as Reynolds number, Mach number and whether the flow is laminar or turbulent. It should be mentioned that in small Reynolds numbers, the drag force applied to the particles is proportional to the size of the particles and the difference between the velocity of the flame and the particle. At low Reynolds numbers, the drag force on a rigid sphere of radius r_p is given by Stokesian approximation as:

$$F_D = -6\pi\mu r_p (v_p - v_f) \quad (3)$$

Where μ and v_f are gas viscosity and the flame propagation velocity in the mixture of micro-particle and the air.

2.1.3. Gravitation and buoyancy forces

The gravitation and Buoyancy forces applied to spherical particles are presented via the following equation.

$$F_G + F_B = -\frac{4}{3}\pi r_p^3 (\rho_p - \rho_g)g \quad (4)$$

Where ρ_p and ρ_g , are the particle and gas densities respectively, and g is the gravitational acceleration vector.

2.1.2. Thermophoretic force

Thermophoretic is a term describing a phenomenon where small particles such as soot particles, aerosol and so on, when suspended in a gas with temperature gradient, can feel this force in the opposite direction to the temperature gradient. This phenomenon was first proved by Aitken, with a series of experiments in 1884, that the dust particles must have been driven away from the heated surface by differential bombardment of the gas molecules [25]. The thermophoretic force should be investigated in most reacting dusty flows, in which particles with diameters of the order of microns or less are flowing against substantial temperature gradients. Talbot et al. [26] presented an acceptable equation in continuum limit of small Knudson numbers for the spherical particles which is presented as:

$$F_T = -6\pi\mu^2 d_p \frac{C_s k_g}{k_p + 2k_g} \frac{\nabla T}{\rho_g T_u} \quad (5)$$

In which ∇T is the temperature gradient in the mixture of micro-iron particles and gas and T_u is the mean gas temperature of the surrounding region of the particles and equal to the temperature of the unburned mixture. In addition, C_s, k_g, k_p are the temperature jump coefficient and thermal conductivity for the gas and particles respectively.

The value 1.147 is suggested for C_s by Batchelor and Shen [27].

2.2. Thermal equations

In order to obtain flame propagation characteristics such as flame velocity and temperature, an analytical model is developed taking the mass and energy conservation equations into account. Besides, to calculate the thermophoretic force, temperature profile of the micro-iron particles-air mixture is needed. In this study, the proposed model is based on a model that has been previously developed by Goroshin et al. [15] and Huang et al. [28] for aluminum dust particles. In addition to the fact that the model has demonstrated good correlation with results obtained using suspensions of small particle sized aluminum dust in air, the model predictions have a good agreement to the experimental results for iron dust particles as shown by Tang et al. [16,21]. In the model, following simplifying assumption are made: 1) The temperature for the particles and the gas is the same and as a result of that, there is no heat transfer between them. 2) Particle distribution for iron in the air is uniform. 3) Biot number is so small that the temperature inside the particle is taken to be uniform. 4) Heat transfer by radiation is ignored. 5) Coefficient of conduction, heat capacity of the mixture, density and burning time for the particles are constant. With these approximations, the governing mass and energy equations describing the preheat and combustion zones become linear and can be solved in closed form. For the steady, one-dimensional, and laminar flame propagation, the mass and energy conservation equations are generally expressed as:

$$\rho v = \rho_u v_f \quad (6)$$

$$\rho v \frac{\partial}{\partial x}(cT) = \frac{\partial}{\partial x} \left(\lambda \frac{\partial T}{\partial x} \right) + \dot{w} q \quad (7)$$

Where \dot{w} is the rate of reaction, q the heat of reaction, v_f the flame velocity. Also, ρ , v , T are the mixture density, velocity, and temperature, respectively.

To solve the conservation equations, structure of flame propagation through iron dust particles is divided into two zones; a preheat zone, and a combustion zone. These equations are solved in these two regions using suitable boundary conditions, and since convection heat losses to the walls is ignored because of the special design of combustion chamber, it is assumed the flame temperature gets stable after its maximum value. Accordingly, the boundary conditions can be expressed as:

$$x \rightarrow -\infty, \quad T_I = T_u$$

$$x = 0, \quad T_I = T_{II}$$

$$\begin{aligned}
 x = 0, \quad & \frac{\partial T_I}{\partial x} = \frac{\partial T_{II}}{\partial x} \\
 x \rightarrow +\infty, \quad & \frac{\partial T_{II}}{\partial x} = 0
 \end{aligned} \quad (8)$$

Here T_u represents the temperature of unburned mixture, and T_I , T_{II} show the temperature in the preheat and combustion zones respectively. Also, $x = 0$ indicates the leading edge of the combustion zone.

III. Analytical solution

3.1. Thermal equations

Introduce the non-dimensional variables and parameters as follows:

$$\theta = \frac{T - T_u}{T_i - T_u}, \quad X = \frac{x}{v_f \tau_c}, \quad S^2 = \frac{\rho_u c v_f^2 \tau_c}{\lambda}, \quad \gamma = C_{d,u} \frac{q}{\rho_u c (T_i - T_u)} \quad (9)$$

Where T_i represents the ignition temperature of micro-iron particles, and τ_c is the particle burning time. Also, $C_{d,u}$ is the initial mass concentration of particulate fuel and equal to the concentration of particles in the unburned mixture.

$S = \frac{v_f}{(\lambda / \rho_u c \tau_c)^{1/2}}$ is the dimensionless flame velocity, and γ is the dimensionless heat release. In this model, rate of reaction $\dot{w} = (C_{d,u} / \tau_c) \exp(-X)$ is taken into account according to the amount of fuel available (initial mass concentration of fuel), and the total particle burning time which is assumed to be equal to the burning time of a single particle [15]. Substituting the above parameters into equations (7) and (8), we obtain the following non-dimensional equations and boundary conditions for the two different zones.

Preheat zone:

$$\frac{\partial^2 \theta_I}{\partial X^2} - S^2 \frac{\partial \theta_I}{\partial X} = 0 \quad (10)$$

Combustion zone:

$$\frac{\partial^2 \theta_{II}}{\partial X^2} - S^2 \frac{\partial \theta_{II}}{\partial X} + S^2 \gamma \exp(-X) = 0 \quad (11)$$

Dimensionless boundary conditions are:

$$\begin{aligned}
 X \rightarrow -\infty, \quad & \theta_I = 0 \\
 X = 0, \quad & \theta_I = \theta_{II} \\
 X = 0, \quad & \frac{\partial \theta_I}{\partial x} = \frac{\partial \theta_{II}}{\partial x} \\
 X \rightarrow +\infty, \quad & \frac{\partial \theta_{II}}{\partial x} = 0
 \end{aligned} \quad (12)$$

By solving thermal equations (10) and (11), applying suitable boundary conditions (12), dimensionless temperature equations as a function of dimensionless space can be calculated in two zones.

Preheat zone:

$$\theta_I(X) = \frac{\gamma}{S^2 + 1} \exp(S^2 X) \quad (13)$$

Combustion zone:

$$\theta_{II}(X) = \gamma - \frac{S^2 \gamma}{S^2 + 1} \exp(-X) \quad (14)$$

At the leading edge of the combustion zone $x = 0$, the particles reach their ignition temperature T_i . Taking this condition into temperature profile equations leads to the following correlation for the flame velocity.

$$v_f^2 = \frac{\lambda}{\rho_u c \tau_c} \left(C_{d,u} \frac{q}{\rho_u c (T_i - T_u)} - 1 \right) \quad (15)$$

The last equation agrees fairly well with the general remarks in literature [29,30], where for a flame propagating via molecular transport of heat, dimensional analysis suggested that the propagation velocity v_f should depend on the thermal diffusivity α and the characteristic combustion time τ_c as follows: $v_f^2 \sim \alpha / \tau_c$.

3.2. Dynamic equations of particles

In order to solve the dynamic equations, the distance between the particles and the leading edge of the flame is presented by $x_{rel} = x_p - x_f$, and the velocity of the particles toward the edge of the flame with $v_{rel} = v_p - v_f$. Substituting equations (3), (4) and (5) into equation (2), and by applying the abovementioned relative position and velocity, the following differential equations are achieved to calculate particles velocity.

$$\left(\frac{4}{3} \pi r_p^3 \rho_p \right) \frac{dx_{rel}^2}{dt^2} = - \left(6 \pi \mu r_p \right) \frac{dx_{rel}}{dt} + F_T - \frac{4}{3} \pi r_p^3 \rho_p \left(1 - \frac{\rho_g}{\rho_p} \right) g \quad (16)$$

As the value of thermophoretic force is proportional to the temperature gradient according to equation (5), and considering the temperature profile, obtained in the preheat zone from equation (13), it can be calculated as follows:

$$F_T(x) = -6 \pi \mu^2 d_p \frac{C_s k_g}{k_p + 2k_g} \frac{1}{\rho_g T_u} \left(\frac{T_i - T_u}{v_f \tau_u} \right) \frac{\gamma S^2}{S^2 + 1} \exp \left(\left(\frac{S^2}{v_f \tau} \right) x \right) \quad (17)$$

Using equations (13) and (14), the temperature profile is depicted in figure (2a). As observed in figure (2a), maximum value of the temperature gradient is at the edge of the

flame $x = 0$. Consequently, thermophoretic force is significant only at this location and the amount of this force tends to zero by getting farther than the edge of the flame, figure (2b). Since the concentration which the edge of flame senses plays a key role during the flame propagation, it is assumed that the value of thermophoretic force has a constant value, and it equals its value at the edge of the flame. As a result, by solving the ordinary differential equation (16), the correlation of relative position as a function of time is acquired as:

$$x_{rel} = c_1 \exp \left[\left(-\frac{9\mu}{2r_p^2 \rho_p} \right) t \right] + c_2 + \left[\frac{F_T}{(6\pi\mu r_p)} - \left(\frac{2r_p^2 \rho_p}{9\mu} \right) \left(1 - \frac{\rho_g}{\rho_p} \right) g \right] t \quad (18)$$

Moreover, the equation of relative velocity of the particles as a function of time is obtained using the coming approach:

$$v_{rel} = \frac{dx_{rel}}{dt} = c_1 \left(-\frac{9\mu}{2r_p^2 \rho_p} \right) \exp \left[\left(-\frac{9\mu}{2r_p^2 \rho_p} \right) t \right] + \left[\frac{F_T}{(6\pi\mu r_p)} - \left(\frac{2r_p^2 \rho_p}{9\mu} \right) \left(1 - \frac{\rho_g}{\rho_p} \right) g \right] \quad (19)$$

To obtain the constants c_1 and c_2 , two time conditions are required. In fact, particles are only influenced by gravitation and Buoyancy forces at a certain distance L_t , and move downward with the constant velocity U_t . In fact, L_t is a characteristic length of a zone in front of the flame in which particles have not sensed the effects of the flame yet. The amount of U_t is calculated by balancing drag, Buoyancy and gravitation forces as:

$$U_t = \frac{2}{9} \frac{gr_p^2}{\mu} (\rho_p - \rho_g) \quad (20)$$

Supposing that the particles, at the initial moment, are at the distance L_t from the edge of the flame, two initial conditions can be expressed as:

$$x_{rel}(t=0) = L_t \quad (21)$$

$$v_{rel}(t=0) = -U_t - v_f \quad (22)$$

By applying the initial condition (22) in equation (19), the value of c_1 is gained this way:

$$c_1 = \left(\frac{2r_p^2 \rho_p}{9\mu} \right) \left(v_f + \frac{F_T}{(6\pi\mu r_p)} \right) \quad (23)$$

Ultimately, by inserting equation (23) in equation (18) and applying the initial condition (21), the value of c_2 can be obtained using the following equation.

$$c_2 = L_t - \left(\frac{2r_p^2 \rho_p}{9\mu} \right) \left(v_f + \frac{F_T}{(6\pi\mu r_p)} \right) \quad (24)$$

3.3. Mass concentration of particles

By determining the position and velocity of the particle as a function of time for iron particles, the number density profile of particles in the preheat zone can be calculated. In order to reach the number density profile of particles in front of the flame, a small enough control volume above the leading edge of combustion zone is assumed, figure (3). This volume control is located at the distance value of x from the edge of the flame and has the height value of Δx and area value of A . Supposing that the particles move vertically along with the duct axes, when passing the volume control, the variation in the number density of particles can be calculated by balancing particle mass fluxes.

For the condensed phase, fractional volume is determined as the proportion of particles volume to the total volume. For the condensed phase of particles, the fractional volume is defined as $\psi = C_d / \rho_p = n_s m_p / \rho_p$. Where C_d is the mass concentration of particulate fuel, and n_s is the number density of particles (i.e., the number of particles in the volumetric unit). The particles mass flux passing through a volume control is equal to $\rho_p A v_{rel} \psi$ and taking Δx as the height of volume control, flux variation at x axis is:

$$\frac{\partial \rho_p A v_{rel} \psi}{\partial x} \Delta x = \frac{\partial \rho_p v_{rel} \psi}{\partial x} A \Delta x \quad (25)$$

In which $v_{rel} = v_p - v_f$ is the relative velocity of the particles which is determined in the equations (19). The accumulation rate of particles is $(\partial(\rho_p \psi) / \partial t) A \Delta x$, and since there is no mass reduction in the iron particle combustion as a result of gasification, the mass equation for the volume control is expressed as follows:

$$\frac{\partial(\rho_p \psi)}{\partial t} A \Delta x = \frac{\partial \rho_p v_{rel} \psi}{\partial x} A \Delta x \quad (26)$$

Solving the above equation with the boundary condition $x = L_t \rightarrow \psi = \tilde{\psi}$, the values for the ratio of the fractional volume and ratio of number density of particles would be as follows:

$$\frac{\psi}{\tilde{\psi}} = \frac{n_s}{\tilde{n}_s} = \frac{\tilde{v}_{rel}}{v_{rel}} \quad (27)$$

Where $\tilde{\psi} = C_{d,u} / \rho_p = \tilde{n}_s m_p / \rho_p$. Also, \tilde{n}_s , and \tilde{v}_{rel} are the number of particles in the

volumetric unit and the relative velocity of particles at $x = L_t$. Therefore, actual concentration of the iron dust cloud (i.e., the concentration which the edge of flame senses during flame propagation) can be written as follow:

$$C_{d,act} = \frac{\tilde{v}_{rel} \cdot C_{d,u}}{c_1 \left(-\frac{9\mu}{2r_p^2 \rho_p} \right) \exp \left[\left(-\frac{9\mu}{2r_p^2 \rho_p} \right) t_1 \right] + \left[\frac{F_T}{(6\pi\mu r_p)} - \left(\frac{2r_p^2 \rho_p}{9\mu} \right) \left(1 - \frac{\rho_g}{\rho_p} \right) g \right]} \quad (28)$$

Where t_1 is the time when particles reach the leading edge of flame $x = 0$, and it can be obtained from equation (18). Also, c_1 is gained from equation (23).

IV. Results and discussion

The major goal of this article is to study the dynamic behavior of micro-iron particles in the preheat zone and its impact on the flame propagation characteristics. The preheat zone is affected by the combustion zone and causes the difference in the velocity of the two phases of solid and gas. This difference can change number density of particles at the leading edge of the combustion zone. The analytical results have been compared with the experimental work done by Sun et al. [7,8].

Figure (4a) illustrates the distance of the iron particles from the leading edge of the combustion zone through time using equation (18). At $t = 0$ the position of particles are L_t , and as it is obvious, with increasing the mass concentration of micro-iron particles, the time for the particles to reach the edge of the flame decreases. It is worth noting that in the experimental study carried out for determining the density and velocity profiles of iron particles by Sun et al. [8], the quantity of L_t was reported around 10 mm at the constant $v_f = 25 \text{ cm/s}$ and $C_{d,u} = 1.05 \text{ kg/m}^3$. Figure (4b) displays variation in the particles velocity for different mass concentration using equation (19). According to the diagram, as the particles move closer to the edge of the flame considering the effect of the combustion zone, their velocity decreases from about $U_t = 11.5 \text{ cm/s}$ to zero in the direction opposite to the flame propagation direction. And then, their velocity increases until they reach the leading edge of the flame. The flame velocities required for equations are determined from equation (15).

The velocity profile for the micro-iron particles for $C_{d,u} = 1.05 \text{ kg/m}^3$ is described in figure (5) which indicates that the velocity of the particles can change by the distance to the leading

edge of the flame. It should be mentioned that, particles before reaching the characteristic length L_t move with constant velocity U_t . As soon as they reach the certain distance L_t , their velocity decline and tend to zero. As they pass approximately half of the length, they take the opposite direction and their velocity increases until they reach the leading edge of the flame. The results are compared with previous experimental results [8].

In figure (6), the ratio of fractional volume $\psi/\tilde{\psi}$ based on the distance from the edge of the flame is depicted using equation (27). As expected, the relative velocity between the particles and the flame results in the accumulation of the particles in the preheat zone and especially on the edge of the flame. This process makes the flame move in a denser environment and has effects on the reaction rate of particles and flammability limit in this mixture. The results are compared with previous experimental results [8].

Table (1) is reported the value of most significant parameters involved in the laminar flame propagating in suspensions of iron dust in air, and the corresponding actual concentration, obtained by virtue of equation (28). In this table, t_1 is obtained from equation (18). Besides, values of flame velocity v_f , and actual flame velocity $v_{f,act}$ are gained by putting $C_{d,u}$, and $C_{d,act}$ in equation (15). It is worth mentioning that $\omega = C_{d,act}/C_{d,u}$ is a correction factor which indicates that flame moves in a denser environment compared to the initial condition.

Figure (7) illustrates the effect of the mass concentration of particles on the laminar flame velocity for the iron dust cloud. In general, trends of the v_f , and $v_{f,act}$ are slightly upward; In fact, with a rise in the concentration of the dust cloud from about 0.5 kg/m^3 to about 1.05 kg/m^3 , the flame propagates more rapidly. The calculations were accomplished by putting $\omega = 2.2$ as an average amount of the correction factor. It can be easily observed that the deviation between calculated value and experimental data result [7], can be considered adequate for $v_{f,act}$ in comparison with v_f . Hence, $C_{d,act}$ seems more useful than $C_{d,u}$ to obtain more realistic estimates of the laminar flame velocity propagating in suspensions of iron dust in air.

V. Conclusions

As the analytical results of the present study show, contrary to the developed theory of homogeneous gas flames, flame propagation in the micro-iron dust particles is largely under the

influence of particle motions as well as heat and mass transfer. At the time of flame propagation, the velocity of the gas increases near the combustion zone as a result of expansion, and leads to creation of a slip between two phases. Consequently, the particles concentration in the preheat zone is affected and results in the change in the flame velocity. Results show the mass concentration of the particles in the preheat zone changes and gets larger until it reaches the maximum value in the leading edge of the flame. It can be observed that actual mass concentration, presented in this paper, seems to be much more useful than initial mass concentration of the mixture to obtain more realistic estimates of the flame velocity propagating in suspensions of micro-iron dust particles in air.

This study proves the importance of conducting more researches on the interphase slipping in a heterogeneous combustion, which directly affects the flame propagation characteristics in a heterogeneous medium. This phenomenon seems to be one of the main reasons why the lower flammability limit of dust cloud flame is much smaller than that of gas fuel flame, and further effort is clearly needed to develop the heterogeneous combustion theory. It is worth noticing that the present approach can be easily adapted to investigate the flame propagation characteristics of different dust clouds such as aluminum, magnesium, lycopodium, woods and biomass.

References

- [1] G. Joseph, CSB Hazard Investigation Team, Combustible dusts: A serious industrial hazard, *J. Hazard. Mater.* 142 (2007) 589-591.
- [2] O. Dufaud, L. Perrin, M. Traore, S. Chazelet, D. Thomas, Explosions of vapour/dust hybrid mixtures: a particular class, *Powder Technology* 190 (2009) 269-273.
- [3] A. Garcia-Agreda, A. Di Benedetto, P. Russo, E. Salzano, R. Sanchirico, Dust/gas mixtures explosion regimes, *Powder Technology* 205 (2011) 81-86.
- [4] W. Gao, R. Dobashi, T. Mogi, J. Sun, X. Shen, Effects of particle characteristics on flame propagation behavior during organic dust explosions in a half-closed chamber, *J. Loss Prev. Process Ind.* 25 (2012) 993-999.
- [5] D.B. Beach, A.J. Rondinone, B.G. Sumpter, S.D. Labinov, R.K. Richards, Solid-state combustion of metallic nanoparticles: new possibilities for an alternative energy carrier, *J. Energy Resour. Technol.* 129 (2007) 29-32.
- [6] J.H. Sun, R. Dobashi, T. Hirano, Combustion behavior of iron particles suspended in air, *Combust. Sci. Technol.* 150 (2000) 99-114.
- [7] J.H. Sun, R. Dobashi, T. Hirano, Temperature profile across the combustion zone propagating through an iron particle cloud, *J. Loss Prev. Process Ind.* 14 (2001) 463-467.
- [8] J.H. Sun, R. Dobashi, T. Hirano, Concentration profile of particles across a flame propagating through an iron particle cloud, *Combust. Flame* 134 (2003) 381-387.
- [9] J.H. Sun, R. Dobashi, T. Hirano, Velocity and number density profiles of particles across upward and downward flame propagating through iron particle clouds, *J. Loss Prev. Process Ind.* 19 (2006) 135-141.
- [10] K.L. Cashdollar, Overview of dust explosibility characteristics, *J. Loss Prev. Process Ind.* 13 (2000) 183-199.
- [11] K.L. Cashdollar, I.A. Zlochower, Explosion temperatures and pressures of metals and other elemental dust clouds, *J. Loss Prev. Process Ind.* 20 (2007) 337-348.
- [12] P. Kosinski, R. Nyheim, V. Asokan, T. Skjold, Explosions of carbon black and propane hybrid mixtures, *J. Loss Prev. Process Ind.* 26 (2013) 45-51.
- [13] R.H. Essenhigh, J. Csaba, The thermal radiation theory for plane flame propagation in coal dust clouds, *Symp. (International) Combust.* 9 (1963) 111-125.
- [14] K. Seshadry, A.L. Berlad, V. Tangirala, The structure of premixed particle-cloud flames, *Combust. Flame* 89 (1992) 333-342.
- [15] S. Goroshin, M. Bidabadi, J.H.S. Lee, Quenching Distance of Laminar Flame in Aluminum Dust Clouds, *Combust. Flame* 105 (1996) 147-160.
- [16] F.D. Tang, S. Goroshin, A. Higgins, J. Lee, Flame propagation and quenching in iron dust clouds, *Proc. Combust. Inst.* 32 (2009) 1905-1912.
- [17] M. Broumand, M. Bidabadi, Modeling combustion of micron-sized iron dust particles during flame propagation in a vertical duct, *Fire Safety Journal* 59 (2013) 88-93.
- [18] P.B. Vainshtein, R.I. Nigmatulin, Combustion of gas-particle mixture, *Prikl. Mech. Tech. Phys. (in Russian)* 4 (1971) 19-33.
- [19] E.L. Dreizin, V.K. Hoffman, Constant pressure combustion of aerosol of coarse magnesium particles in microgravity, *Combust. Flame* 118 (1999) 262-280.
- [20] R.A. Yetter, G.A. Risha, S.F. Son, Metal particle combustion and nanotechnology, *Proc. Combust. Inst.* 32 (2009) 1819-1838.
- [21] F.D. Tang, S. Goroshin, A. Higgins, Modes of particle combustion in iron dust flames, *Proc. Combust. Inst.* 33 (2011) 1975-1982.

- [22] C. Proust, Flame propagation and combustion in some dust-air mixtures, *J. Loss Prev. Process Ind.* 19 (2006) 89–100.
- [23] O.S. Han, M. Yashima, T. Matsuda, H. Matsui, A. Miyake, T. Ogawa, A study of flame propagation mechanisms in lycopodium dust clouds based on dust particles behavior, *J. Loss Prev. Process Ind.* 14 (2001) 153–160.
- [24] M.G. Andac, On the structure and dynamics of dusty reacting flows at normal and micro-gravity, PhD Thesis, University Of Southern California, 2002.
- [25] F. Zheng, Thermophoresis of spherical and non-spherical particles: a review of theories and experiments, *Advances in Colloid and Interface Science* 97 (2002) 255-278.
- [26] L. Talbot, R.K. Cheng, R.W. Schefer, D.R. Willis, Thermophoresis of particles in a heated boundary layer, *J. Fluid Mech.* 101 (1980) 737-758.
- [27] G.K. Batchelor, C. Shen, Thermophoretic deposition of particles in gas flowing over cold surfaces, *J. Colloid Interface Sci.* 107 (1985) 21–37.
- [28] Y. Huang, G.A. Risha, V. Yang, R.A. Yetter, Effect of particle size on combustion of aluminum particle dust in air, *Combust. Flame* 156 (2009) 5–13.
- [29] L.D. Landau, E.M. Lifshitz, *Fluid Mechanics*, Pergamon Press, 1987.
- [30] L.P. Yarin, G. Hetsroni, *Combustion of two-phase reactive media*, Berlin: Springer, 2004.

Figures

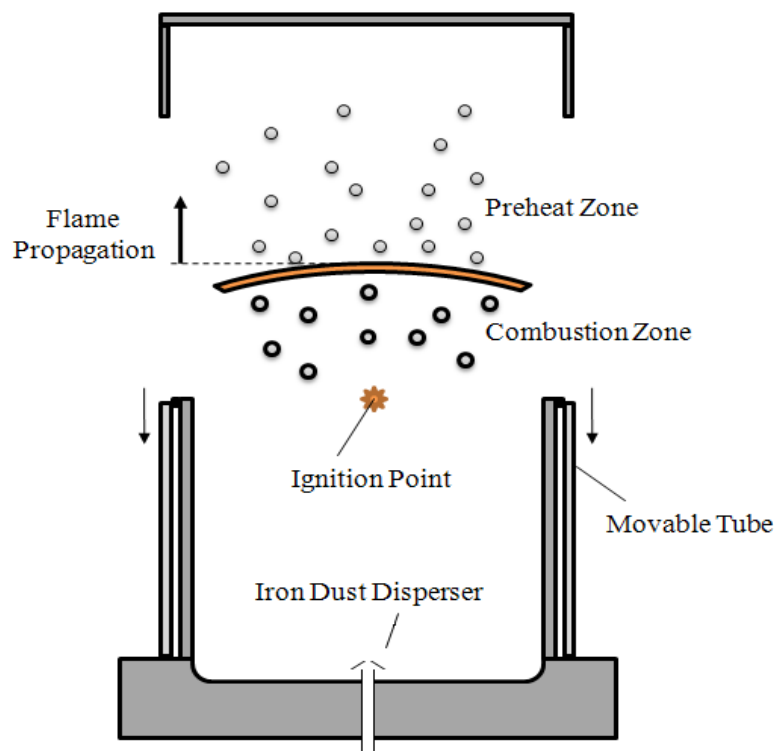


Fig. 1. Flame structure of the combustible mixture of micro-iron dust particles and air.

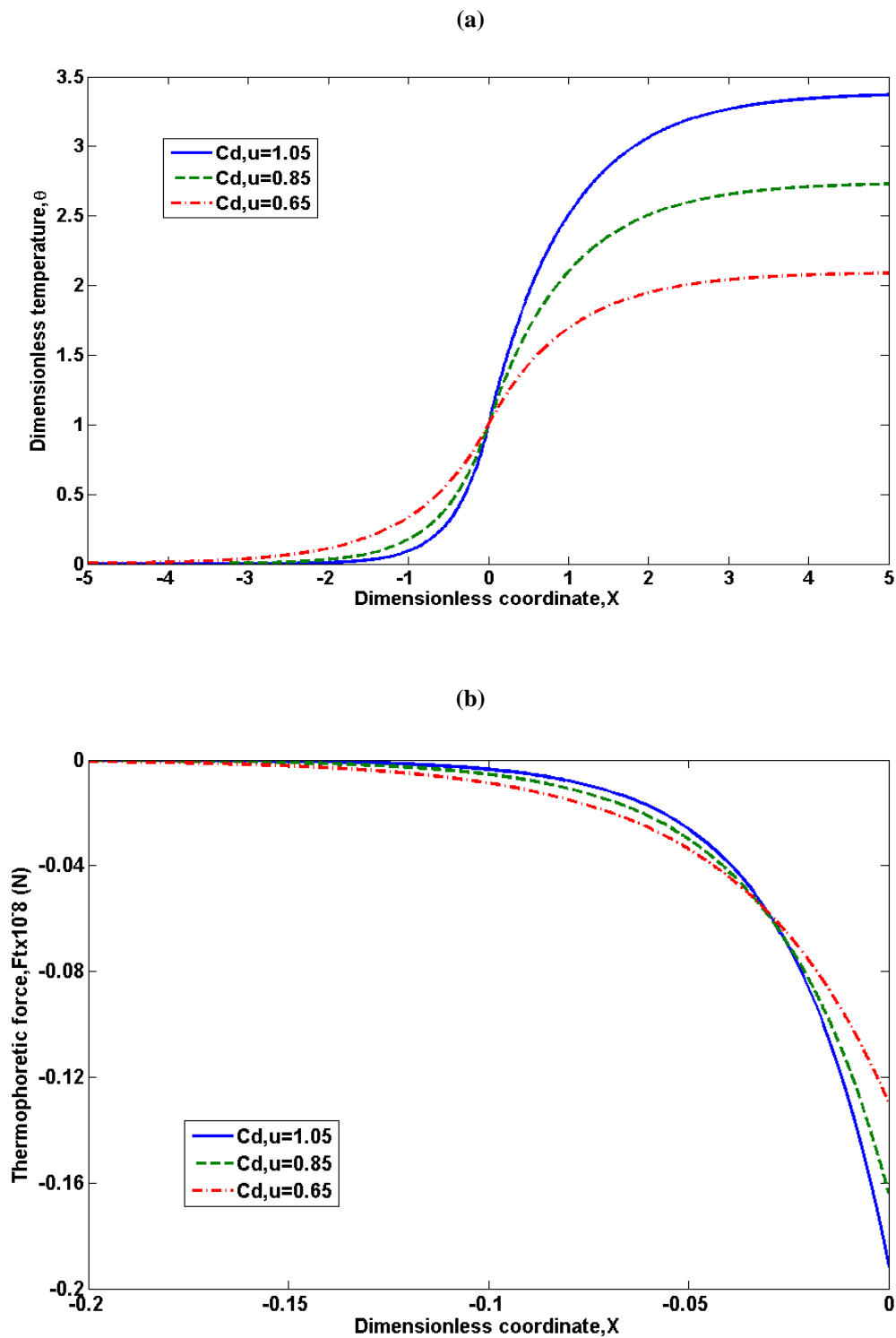


Fig. 2. (a) Dimensionless temperature profile based on the dimensionless coordinate for various mass concentrations. (b) The effect of the variation in the dimensionless coordinate on the thermophoretic force for various mass concentrations.

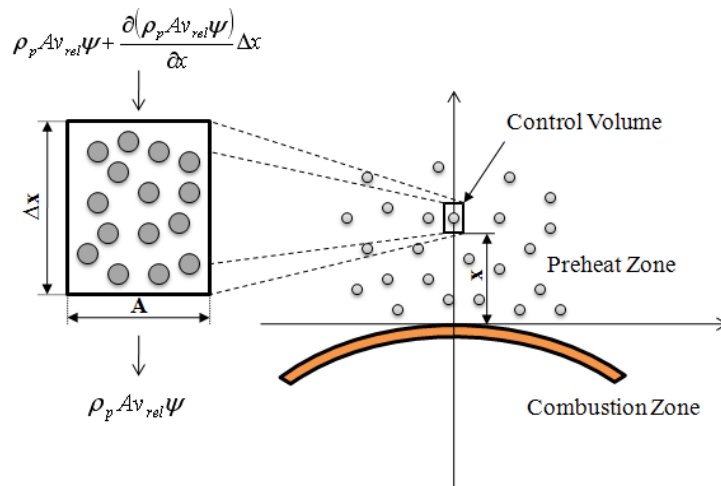


Fig. 3. Control volume on the leading edge of the combustion zone for determining the number density of iron particles.

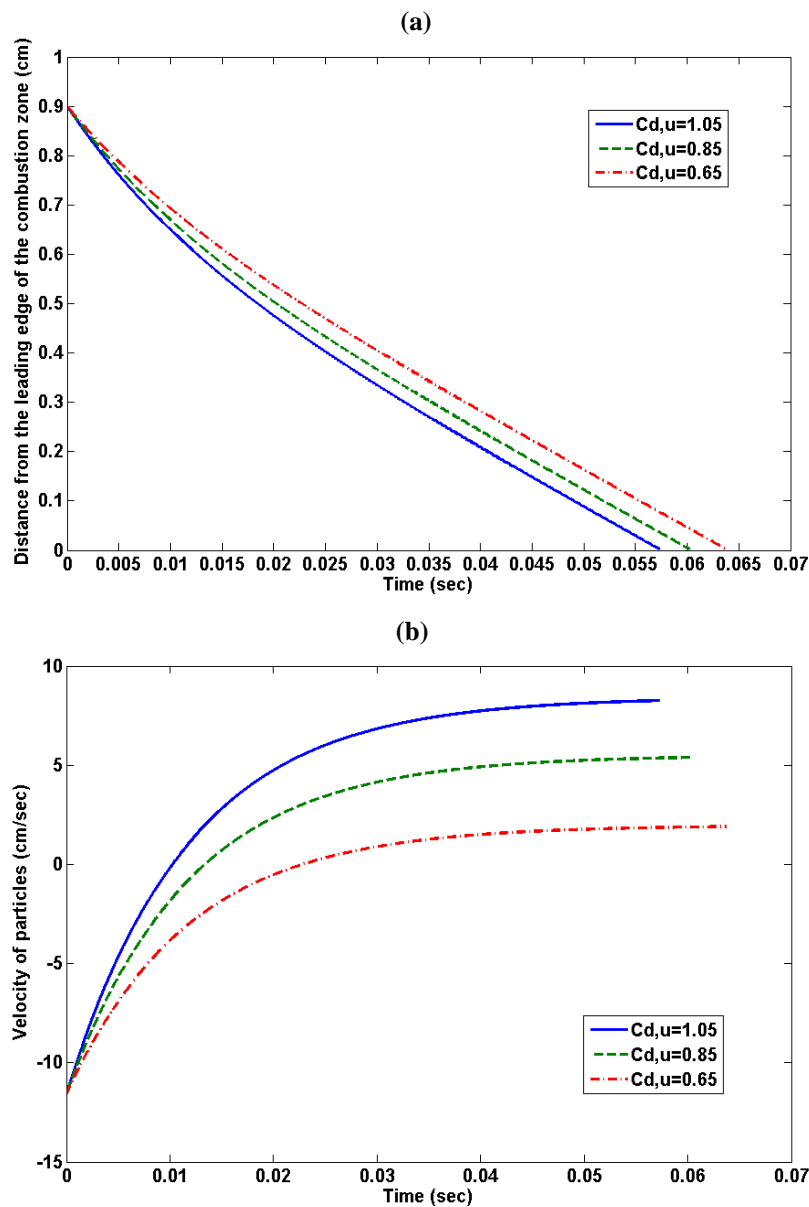


Fig. 4. (a) Particle distances from the leading edge of flame as functions of time for various mass concentrations. (b) Particle velocities as functions of time for various mass concentrations.

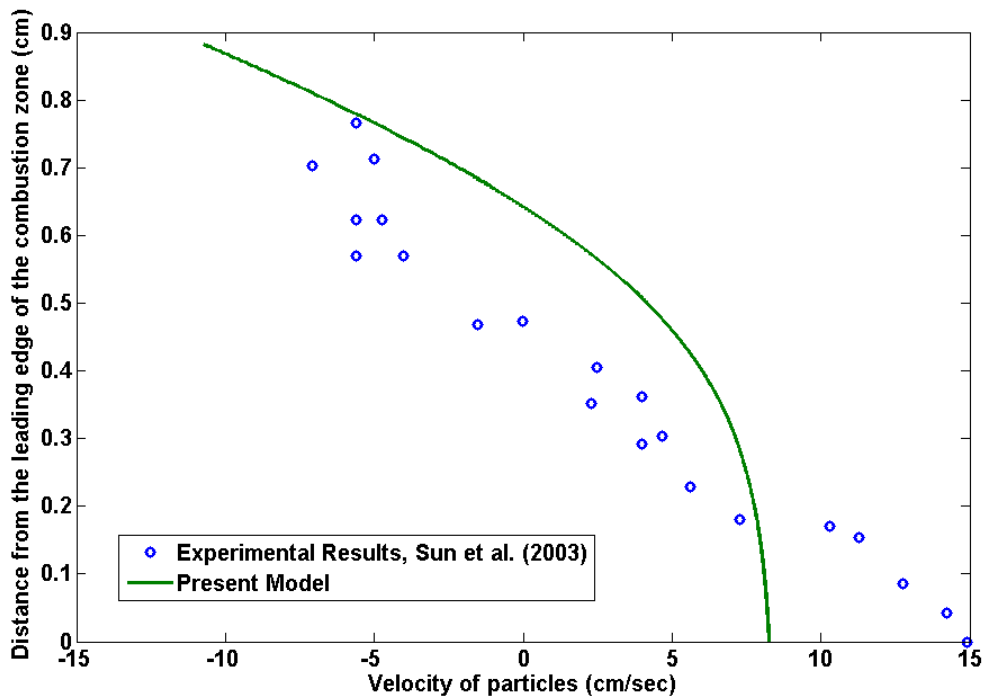


Fig. 5. Comparison of the particle velocity profile across the leading edge of flame obtained from present model with the experimental results [8].

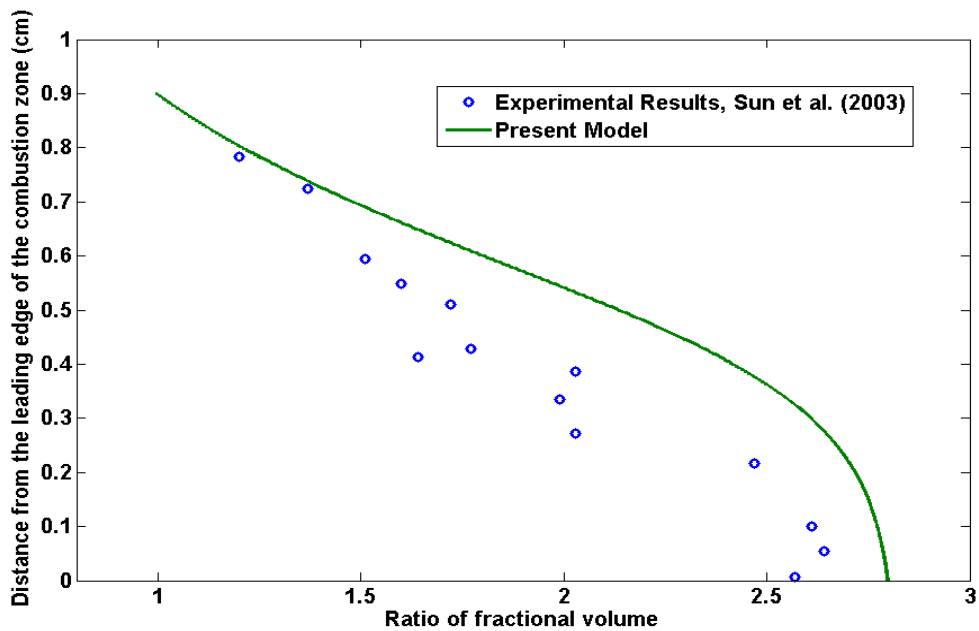


Fig. 6. Comparison of the variation of the fractional volume ratio across the leading edge of flame obtained from present model with the experimental results [8].

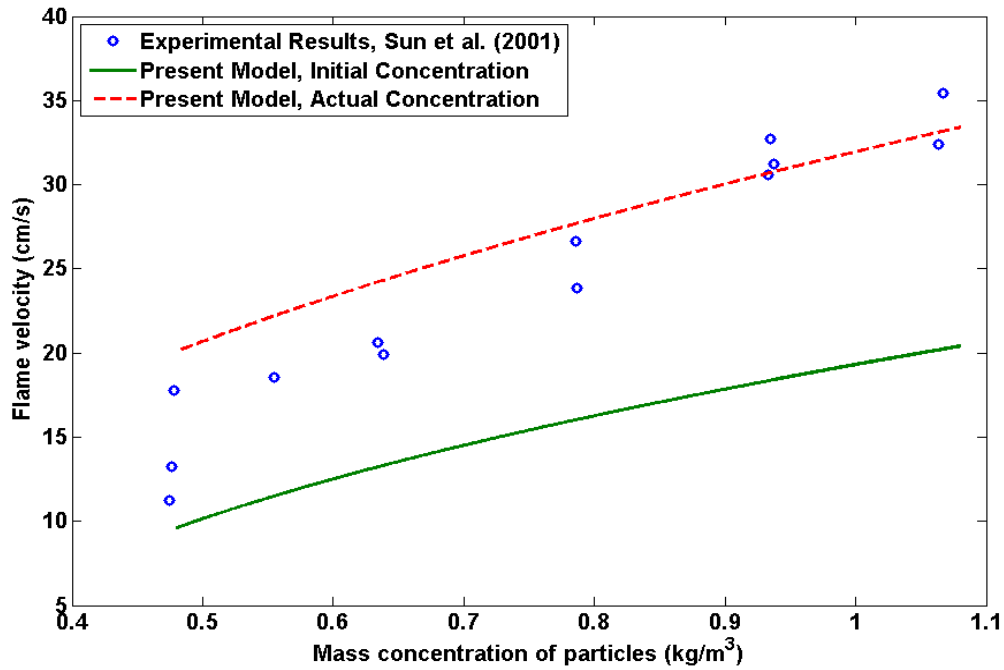


Fig. 7. Comparison of the variation of the laminar flame velocity as functions of initial and actual mass concentration obtained from present model with the experimental results [7].

Table (1)

Characteristics of flame propagation in iron dust particles

$C_{d,u}$ [kg/m ³]	v_f [cm/s]	t_f [ms]	$C_{d,act}$ [kg/m ³]	$v_{f,act}$ [cm/s]	$\omega = C_{d,act}/C_{d,u}$
1.05	20	57.3	2.82	32.88	2.69
0.85	17.08	60.2	2.08	29.03	2.45
0.65	13.55	63.7	1.4	24.6	2.15
0.5	10.13	67.3	0.9343	20.66	1.87